Surface Instability of an Elastic Half Space with Material Properties Varying with Depth

Donghee Lee, Nicolas Triantafyllidis, James R Barber, Michael D Thouless

Published in final edited form as:
J Mech Phys Solids. 2008 ; 56(3): 858–868.

Surface instability of an elastic half space with material properties varying with depth

Donghee Lee[a], **N Triantafyllidis**[b,a], **J.R. Barber**[a,c,*], and **M.D. Thouless**[a,d]

a*Department of Mechanical Engineering, University of Michigan, Ann Arbor, MI 48109-2125, U.S.A.*

b*Department of Aerospace Engineering, University of Michigan, Ann Arbor, MI 48109-2140, U.S.A.*

c*Department of Civil and Environmental Engineering, University of Michigan, Ann Arbor, MI 48109-2125, U.S.A.*

d*Department of Materials Science and Engineering, University of Michigan, Ann Arbor, MI 48109-2136, U.S.A.*

Abstract

If a body with a stiffer surface layer is loaded in compression, a surface wrinkling instability may be developed. A bifurcation analysis is presented for determining the critical load for the onset of wrinkling and the associated wavelength for materials in which the elastic modulus is an arbitrary function of depth. The analysis leads to an eigenvalue problem involving a pair of linear ordinary differential equations with variable coefficients which are discretized and solved using the finite element method.

The method is validated by comparison with classical results for a uniform layer on a dissimilar substrate. Results are then given for materials with exponential and error-function gradation of elastic modulus and for a homogeneous body with thermoelastically-induced compressive stresses.

Keywords

layered materials; stability and bifurcation; inhomogeneous material; buckling; functionally graded material

1 Introduction

If a structure consisting of a thin stiff layer and a more flexible substrate is subjected to a sufficiently large compressive load, a buckling or wrinkling surface instability can occur, as shown in Fig. 1. Generally, surface wrinkling has been considered as an undesirable phenomenon to be avoided. However, in emerging areas such as micro/nano-fabrication and bio-engineering, wrinkling can be used to produce controlled nanoscale features (Bowden *et al.* (1999),Moon *et al.* (2007),Efimenko *et al.* (2005)). It has been proposed that these may be useful for applications such as diffraction gratings, patterned platforms for cell adhesion or nano-fluidic channels. Surface wrinking may also provide a way of probing the surface characteristics of the materials (Stafford *et al.*, 2004).

* Corresponding author. jbarber@umich.edu (J.R.Barber).

Chen and Hutchinson (2004) developed a closed-form solution for the wrinkling of a gold layer deposited on an elastomer substrate. They modeled the structure as a plate on linear elastic foundation with infinite thickess. The same methodology was extended to the case of a thin elastic layer on a substrate of finite thickness by Huang *et al.* (2005). These solutions most naturally relate to the situation in which a thin stiff film is deposited on a more flexible substrate, so that there is a sharp discontinuity in elastic modulus at the interface. However, similar effects should be anticipated in cases where the elastic modulus of the material is graded continuously from the surface to a lower substrate value.

The present work was motivated by observations of micron-scale buckling on oxidized poly (methyldisiloxane)(PDMS) in which a stiff surface-modified layer was formed by exposure to an oxygen plasma. The surface layer in this material is formed by a diffusive process, so we anticipate a gradation of mechanical properties from the surface. The absence in the literature of any discussion of surface wrinkling under these conditions prompted the question of how the mechanics of wrinkling might be affected by the graded properties. The intent of this paper is to establish the general mechanics framework for the study of such problems. In particular, we develop a bifurcation method to analyze the onset of surface wrinkling of an elastic layer with elastic properties that are arbitrary functions of depth. The analysis is sufficiently general to allow for an arbitrary distribution of applied compressive strain with depth. In addition to cases of functionally-graded elastic modulus, it can therefore be applied to situations where a non-uniform distribution of eigenstrain is generated by thermal expansion or other mechanisms such as a change in lattice parameters due to variable concentration of a diffusive species (Larché and Cahn, 1982). The method is validated by comparison with the results of Huang *et al.* (2005). It is then used to determine the critical compressive strain at which wrinkling occurs and the associated wavelength for different distributions of elastic moduli. A subsequent paper will examine some specific examples of buckling associated with cracking in oxidized PDMS.

2 General theory of the instability

The study of buckling (i.e. the sudden change of deformation pattern upon increase of the externally applied load) in elastic structures and solids is a classical problem in solid mechanics, dating back two and a half centuries to Euler and his celebrated study of the problem of the elastica. Restricting attention to conservative elastic systems, the key ingredients for the appearance of buckling are the non-linearity of the system's governing equations and the symmetries inherent in its fundamental solution (i.e. the solution which exists at small load levels, prior to the appearance of buckling). These features are present in the problem at hand, as will be explained below.

For elastic solids, Koiter (1945) was the first in the mechanics community to formulate buckling as a bifurcation problem associated with the principal solution and provide an asymptotic technique to follow the post-bifurcation equilibrium paths. With the development of large strain continuum mechanics in the early 1950's, Koiter's work was subsequently applied to a vast array of structural buckling problems in mechanics. The interested reader is referred to the eminently readable review article by Budiansky (1974), who gives the variational formulation for buckling problems in elastic solids that have a potential energy. The connection between the loss of stability of the principal solution at the lowest load bifurcation in elastic systems — the reason for associating the onset of a bifurcation buckling with an instability in these applications — is also well explained in this article. The most general variational formulation of the buckling and post-buckling problem of conservative elastic systems can be found in Triantafyllidis and Peek (1992), whose notation is followed in the present paper.

We consider the orthotropic elastic layer $0 < x_2 < H_t$ in a state of plane strain and subjected to a compressive load parallel to the x_1 axis, as shown in Fig. 2. The elastic moduli $L_{ijkl}(x_2)$ are assumed to be arbitrary functions of x_2 only, satisfying the major and minor symmetry conditions

$$L_{ijkl}=L_{klij}=L_{jikl}=L_{ijlk}.$$

The boundary $x_2 = 0$ is assumed traction-free, while $x_2 = H_t$ is attached to a rigid plane surface. In many cases, the wrinkling field will be localized near the free surface and we can then use the simplifying assumption that the body is a half space ($H_t \to \infty$) with zero displacement at infinity.

If there is no wrinkling, we expect the stress state to be independent of x_1. We shall refer to this as the 'fundamental stress state' and the corresponding solution of the elasticity equations as the 'principal solution' $\overset{0}{\sigma}$. It must satisfy the equilibrium equations

$$\overset{0}{\sigma}_{ij,i}=0 \quad i,j=1,2$$

and the boundary conditions

$$\overset{0}{\sigma}_{i2}=0$$

on the free surface $x_2 = 0$. Here and subsequently, the notation $(.)_{,i}$ denotes differentiation with respect to x_i and the Einstein summation convention is implied over repeated indexes. Since there is no dependence on x_1 (i.e $\overset{0}{\sigma}_{,1}=0$), the only possible non-zero stresses are $\overset{0}{\sigma}_{11},\overset{0}{\sigma}_{33}$ which can be general functions of x_2. It is convenient to define a loading parameter Λ such that $\overset{0}{\sigma}(x_2,\Lambda)=0$ at $\Lambda = 0$ and an increase in Λ describes a set of progressively increased applied loads. We then anticipate that above some critical value of Λ, the principal solution will become unstable and wrinkling will occur.

2.1 Nature of the loading

The loading $\overset{0}{\sigma}$ may result from a force applied to the extremities of the body, but in this case, compatibility considerations demand that the corresponding strain $\overset{0}{\varepsilon}_{11} \equiv \varepsilon_0$ be independent of x_2, giving

$$\overset{0}{\sigma}_{ij}=L_{ij11}(x_2)\varepsilon_0.$$

Thus, the fundamental stress state varies with depth in proportion with the elastic modulus. However, more general variations in loading can be generated by other mechanisms. For example, if the temperature $T(x_2)$ of the body is a function of depth, we will have

$$\overset{0}{\sigma}_{ij}=L_{ijkl}(x_2)\left\{\overset{0}{\varepsilon}_{kl}-\alpha_{kl}T(x_2)\right\}, \tag{1}$$

where α_{kl} is the tensor of thermal expansion coefficients. This situation may give rise to wrinkling even for a homogeneous half space if the surface is suddenly heated, leading to high compressive stresses in a thin surface layer. Other physical mechanisms leading to transformation strains could have similar effects.

2.2 Analysis

Since we assume an elastic material response, the problem is conservative and a potential energy functional $P(u_i)$ exists, defined by

$$P(u_i) = U_{\text{int}} + W_{\text{ext}} \tag{2}$$

where u_i is the displacement field, U_{int} is the internal energy, and W_{ext} is the potential of the external forces. The latter are given by

$$U_{\text{int}} = \int_V W(\varepsilon_{ij}) dV \quad \text{and} \quad W_{\text{ext}} = -\int_V \rho b_i u_i dV - \int_{\partial V} t_i u_i d\Gamma, \tag{3}$$

where $W(\varepsilon_{ij})$ is the strain energy density in the body V, b_i is the body force and t_i is the traction on the boundary ∂V. In the present problem, there is no body force or boundary traction, so only the strain energy term appears in the subsequent analysis. The strain energy density W is

$$W = \frac{1}{2} L_{\text{ijkl}} \varepsilon_{ij} \varepsilon_{kl}, \tag{4}$$

where ε_{ij} is the strain field. The wrinkling is governed by small strains and moderate rotations, so the strain can be expressed as

$$\varepsilon_{ij} = \frac{1}{2}\left(\frac{\partial u_i}{\partial x_j} + \frac{\partial u_j}{\partial x_i} + \frac{\partial u_k}{\partial x_i}\frac{\partial u_k}{\partial x_j}\right). \tag{5}$$

The equilibrium of this system can be examined by taking the first derivative of the potential energy,

$$P_{,u}\delta u = 0. \tag{6}$$

The equilibrium equation can be expressed in the weak form by substituting equations (2)–(5) into (6), giving

$$\int_V \sigma_{ij} \delta \varepsilon_{ij} dV = 0. \tag{7}$$

The fundamental stress state $\overset{0}{\sigma}(\Lambda)$ is always a solution of Eq. (7).

We now consider the stability of the principal solution by taking the derivative of the equilibrium equation. The principal solution is stable in the neighborhood of $\Lambda = 0$ since it minimizes the total potential energy P — i.e $\left[P_{,uu}\left(\overset{0}{u}\right)\delta u\right]\delta u > 0$, where $\overset{0}{u}(\Lambda)$ is the displacement field corresponding to the fundamental stress state $\overset{0}{\sigma}$ and δu is any kinematically admissible perturbation. As Λ increases, there will be a critical value Λ^c where stability is lost — $\left[P_{,uu}\left(\overset{0}{u}(\Lambda^c)\right)\Delta u\right]\delta u = 0$ (Eq. (7)), where Δu is the eigenmode. By substituting the stress field $\overset{0}{\sigma}_{ij} = L_{\text{ijkl}}\overset{0}{\varepsilon}_{kl}$ into the left hand side of Eq. (7), we can define a stability functional

$$S(\Lambda) \equiv \left[P_{,uu}\left(\overset{0}{u}(\Lambda)\right)\Delta u\right]\delta u = \int_V \left[L_{\text{ijkl}}\Delta\varepsilon_{kl}\delta\varepsilon_{ij} + \overset{0}{\sigma}_{ij}\Delta\delta\varepsilon_{ij}\right] dV, \tag{8}$$

where

$$\Delta\delta\varepsilon_{ij}=\left(\Delta u_{k,i}\delta u_{k,j}\right)_s;\delta\varepsilon_{ij}=\left(\delta u_{i,j}+\overset{0}{u}_{k,i}\delta u_{k,j}\right)_s;\Delta\varepsilon_{ij}=\left(\Delta u_{i,j}+\overset{0}{u}_{k,i}\Delta u_{r,j}\right)_s,$$

where $(.)_s$ denotes the symmetric part of the corresponding second order tensor. Since we assume small strains, $|\overset{0}{u}_{k,i}| \ll 1$ and the strain field perturbation simplifies to $\delta\varepsilon_{ij} \simeq (\delta u_{i,j})_s, \Delta\varepsilon_{ij} \simeq (\Delta u_{i,j})_s$. At the onset of wrinkling, we therefore have

$$S(\Lambda^c)=\left[P_{,uu}\left(\overset{0}{u}(\Lambda^c)\right)\Delta u\right]\delta u=\int_V\left[L_{ijkl}\Delta u_{k,l}\delta u_{i,j}+\overset{c}{\sigma}_{ij}\Delta u_{k,i}\delta u_{k,j}\right]dV=0,, \tag{9}$$

where $\overset{c}{\sigma}\equiv\overset{0}{\sigma}(\Lambda^c)$ Integrating Eq. (9) by parts and using Gauss' divergence theorem, we obtain

$$\left[L_{ijkl}\Delta u_{k,l}+\overset{c}{\sigma}_{pj}\Delta u_{i,p}\right]_{,j}=0, \tag{10}$$

with boundary conditions

$$L_{i2kl}\Delta u_{k,l}+\overset{c}{\sigma}_{p2}\Delta u_{i,p}=0 \tag{11}$$

at the free surface $x_2 = 0$ and

$$\Delta u_i=0 \tag{12}$$

at $x_2 = H_t$.

Since the fundamental stress state $\overset{0}{\sigma}_{ij}$ and the orthotropic elasticity tensor L_{ijkl} are independent of x_1, the equilibrium equation (10) and boundary conditions (11) simplify to

$$\begin{aligned}&L_{1212}\Delta u_{1,22}+L_{1212,2}\Delta u_{1,2}+\left(L_{1111}+\overset{c}{\sigma}_{11}\right)\Delta u_{1,11}+L_{1122}\Delta u_{2,21}+L_{1221}\Delta u_{2,12}\\&+L_{1221,2}\Delta u_{2,1}=0\\&L_{2211}\Delta u_{1,12}+L_{2112}\Delta u_{1,21}+L_{2211,2}\Delta u_{1,1}+L_{2222}\Delta u_{2,22}+L_{2222,2}\Delta u_{2,2}\\&+\left(L_{2121}+\overset{c}{\sigma}_{11}\right)\Delta u_{2,11}=0\end{aligned} \tag{13}$$

$$\begin{aligned}L_{1212}\Delta u_{1,2}+L_{1221}\Delta u_{2,1}=0\\L_{2211}\Delta u_{1,1}+L_{2222}\Delta u_{2,2}=0\end{aligned} \tag{14}$$

respectively. Since the material is orthotropic, equations (13, 12, 14) admit eigenmodes of sinusoidal form

$$\begin{aligned}\Delta u_1=U_1(x_2)\sin(\omega x_1)\\\Delta u_2=U_2(x_2)\cos(\omega x_1).\end{aligned} \tag{15}$$

For the problem at hand, the eigenmode decomposition in (15) is complete. Substituting these expressions into (13), we obtain two ordinary differential equations

$$\begin{aligned}&L_{1212}U_1''+L_{1212}'U_1'-\omega^2\left(L_{1111}+\overset{c}{\sigma}_{11}\right)U_1+\omega\left(L_{1122}+L_{1221}\right)U_2'+\omega L_{1221}'U_2=0\\&L_{2222}U_2''+L_{2222}'U_2'-\omega^2\left(L_{2121}+\overset{c}{\sigma}_{11}\right)U_2-\omega\left(L_{2211}+L_{2112}\right)U_1'-\omega L_{2211}'U_1=0\end{aligned} \tag{16}$$

for the functions $U_1(x_2)$, $U_2(x_2)$, where the primes denotes derivatives with respect to x_2. The boundary conditions are

$$L_{1212}U_1' - \omega L_{1221}U_2 = 0; \quad \omega L_{2211}U_1 - L_{2222}U_2' = 0 \tag{17}$$

at $x_2 = 0$ and

$$U_i = 0 \tag{18}$$

at $x_2 = H_t$, from (14, 15, 12). In the special case where the material is isotropic, equations (16, 17) reduce to

$$\begin{aligned} &\mu U_1'' + \mu' U_1' - \omega^2 \left(\lambda + 2\mu + \overset{0}{\sigma}_{11}\right) U_1 - \omega(\lambda+\mu) U_2' - \omega\mu' U_2 = 0 \\ &\omega(\lambda+\mu) U_1' + \omega\lambda' U_1 + (\lambda+2\mu) U_2'' + (\lambda'+2\mu') U_2' - \omega^2 \left(\mu + \overset{0}{\sigma}_{11}\right) U_2 = 0 \end{aligned} \tag{19}$$

with boundary conditions

$$U_1' - \omega U_2 = 0; \quad \omega\lambda U_1 - (\lambda+2\mu) U_2' = 0 \tag{20}$$

at $x_2 = 0$ and (18) at $x_2 = H_t$, where λ, μ are Lamé's constants.

Equations (16, 17, 18) or (19, 20, 18) define an eigenvalue problem for the critical loading parameter Λ_c and the eigenmodes $U_1(x_2)$, $U_2(x_2)$ for given wavenumber ω. If the elastic modulus L_{ijkl} and the fundamental stress state $\overset{0}{\sigma}$ are piecewise constant functions of x_2, the problem can be solved analytically, but the authors were unable to obtain an analytical solution for the more general case of a functionally-graded material. In the next section, we therefore develop a numerical discretization of the problem.

2.3 Numerical Solution

A numerical solution could be obtained by discretizing the differential equations (16), but it is more convenient to apply the finite element method directly to Eq. (8). Using the same eigenmodes as given in Eq. (15), the stability functional (8) can be written

$$S(\Lambda,\omega) = \int_{x_1}\int_{x_2} \left[L_{ijkl}\Delta u_{k,l}\Delta u_{i,j} + \overset{0}{\sigma}_{ij}\Delta u_{k,i}\Delta u_{k,j} \right] dx_2 dx_1. \tag{21}$$

Stability of the structure depends on $S(\Lambda, \omega)$ being positive definite for all $\omega \in R$. Since from symmetry S depends on ω^2, only $\omega > 0$ needs to be checked for Λ.

The x_2 domain is decomposed in a set of 2-node linear interpolation elements, within each of which the unknown displacement U_i is represented in the form

$$U_i(x_2) = \sum_{I=1}^{2} N_I(x_2) u_i^I, \tag{22}$$

where $N_I(x_2)$ is the shape function and u_i^I is the local degree of freedom for U_i at the two terminal nodes ($I = 1, 2$) of the element. For each element there are therefore four degrees of freedom, which we combine into the vector

$$q_e = \left\{u_1^1, u_2^1, u_1^2, u_2^2\right\}^T.$$

By substituting Eq. (22) into Eq. (21) and integrating over the element in question in x_2-space [1], we obtain the element stiffness matrix

$$\mathrm{k}_e=\int_e \mathrm{L}dx_2,$$

where

$$\mathrm{L}=\begin{bmatrix} \omega^2\left(L_{1111}+\overset{0}{\sigma}_{11}\right) & \omega(L_{1122}-L_{1221}) & \omega^2\left(L_{1111}+\overset{0}{\sigma}_{11}\right) & \omega(L_{1122}N_1N_2' \\ N_1N_1+L_{1212}N_1'N_1' & N_1N_1' & N_1N_2+L_{1212}N_1'N_2' & -L_{1221}N_1'N_2) \\ \omega(L_{2211}-L_{2112}) & \omega^2\left(L_{2121}+\overset{0}{\sigma}_{11}\right) & \omega(-L_{2112}N_1N_2' & \omega^2\left(L_{2121}+\overset{0}{\sigma}_{11}\right) \\ N_1N_1' & N_1N_1+L_{2222}N_1'N_1' & +L_{2211}N_1'N_2) & N_1N_2+L_{2222}N_1'N_2' \\ \omega^2\left(L_{1111}+\overset{0}{\sigma}_{11}\right) & \omega(-L_{1221}N_1N_2' & \omega^2\left(L_{1111}+\overset{0}{\sigma}_{11}\right) & \omega(L_{1122}-L_{1221}) \\ N_1N_2+L_{1212}N_1'N_2' & +L_{1122}N_1'N_2) & N_2N_2+L_{1212}N_2'N_2' & N_2N_2' \\ \omega(L_{2211}N_1N_2' & \omega^2\left(L_{2121}+\overset{0}{\sigma}_{11}\right) & \omega(L_{2211}-L_{2112}) & \omega^2\left(L_{2121}+\overset{0}{\sigma}_{11}\right) \\ -L_{2112}N_1'N_2) & N_1N_2+L_{2222}N_1'N_2' & N_2N_2' & N_2N_2+L_{2222}N_2'N_2' \end{bmatrix}$$

The global stiffness matrix $\boldsymbol{K}$ can then be constructed by adding the element stiffnesses such that

$$\sum_e \mathrm{q}_\mathrm{e}^T\mathrm{k}_\mathrm{e}\mathrm{q}_\mathrm{e}=\mathrm{Q}^T\mathrm{KQ}$$

where $\boldsymbol{Q}$ is a vector of global degrees of freedom. The eigenvalues of the system can be obtained by decomposing the global stiffness matrix $\boldsymbol{K}$ using Choleski decomposition, subject to the essential boundary condition $U_i(H_t) = 0$. We write

$$\mathrm{K}=\mathrm{LDU},$$

where $\boldsymbol{L}$ is the lower triangular matrix with unit diagonal terms, $\boldsymbol{U} = \boldsymbol{L}^T$ is the upper diagonal matrix and $\boldsymbol{D}$ is the diagonal matrix. By tracking the positive definiteness of the matrix **D**, the system stability can be evaluated. If the system is stable, the lowest eigenvalue should be positive. When the load parameter Λ reaches a critical value Λ^c at which the lowest element of $\boldsymbol{D}$ is zero, the system becomes unstable.

3 Results

3.1 Convergence and validation

The method developed in the preceding two sections can be used to evaluate the stability of a layer or half space with arbitrarily graded properties and applied loading. However, to validate the method, we first compare its predictions with the results of Huang *et al.* (2005) for an isotropic homogeneous layer of thickness H_f on a dissimilar substrate of finite thickness H_s (so in our notation $H_t = H_f + H_s$). Notice that these authors made the simplifying assumption that the shear stress at the film/substrate interface remains zero in the buckled state, whereas our analysis is exact within the context of the numerical discretization.

[1]The integral $\int_{x_1}\cos^2(\omega x_1)dx_1=\int_{x_1}\sin^2(\omega x_1)dx_1$ is taken out of (21) as a common factor.

Fig. 3 shows the critical strain ε_0^c and critical dimensionless wavelength $2\pi/\omega^c H_f$ as a function of the thickness ratio H_s/H_f for three values of the modulus ratio $\overline{E}_f/\overline{E}_s$, where $\bar{E}$ is the plane strain modulus defined as

$$\overline{E}=\frac{E}{(1-\nu^2)}$$

and E, ν are Young's modulus and Poisson's ratio respectively. Poisson's ratio for both film and substrate was taken as $\nu = 0.4$. The solid lines are taken from Huang *et al.* (2005) and reproduce their Fig. 5, while the points were obtained from the present program. The agreement is extremely good in all cases.

Tests were also conducted to determine the number of elements required for the numerical solution to converge. A finer mesh was used in the film and in the upper layers of the substrate since the perturbation is concentrated in this region. Better than 0.1% accuracy was obtained using 100 elements in the film and an equal number in a region of the substrate adjacent to the interface of thickness $3H_f$. For the most efficient meshing, the element gradation should follow the rate of decay of the eigenmode, but this depends on the wavelength which is only known *a posteriori*.

It is clear from Fig. 3 and from heuristic considerations that the thickness of the substrate has little effect on the results if it is large compared with the wavelength of the eigenmode. For the homogeneous layer, we found that the half space results can be recovered from the necessarily finite numerical model provided that the substrate thickness H_s is greater than about twice the wavelength — i.e. $H_s > 4\pi/\omega^c$.

3.2 Graded materials

We next turn our attention to continuously graded materials, for which no previous results are available. We considered two examples: a half space in which the plane strain modulus is graded exponentially from a surface value $\bar{E}_0$ to a substrate value $\bar{E}_s$ as $x_2 \to \infty$ — i.e.

$$\overline{E}(x_2)=\overline{E}_s+(\overline{E}_0-\overline{E}_s)\exp\left(\frac{-x_2}{H}\right)$$

and one in which the grading follows the complementary error function

$$\overline{E}(x_2)=\overline{E}_s+(\overline{E}_0-\overline{E}_s)\operatorname{erfc}\left(\frac{x_2}{H}\right). \tag{23}$$

In both of these examples, the parameter H serves as a characteristic length for the decay and can also be used in constructing an expression for the critical dimensionless wavenumber $\omega^c H$. The two expressions are compared in Fig. 4, which shows that the error function decays to zero more rapidly at large depths.

Fig. 5 shows the critical strain ε_0^c and the critical dimensionless wavenumber $\omega^c H$ for the exponentially graded modulus as a function of the modulus ratio $\overline{E}_0/\overline{E}_s$. Poisson's ratio was taken as a constant $\nu = 0.4$ for these calculations. For comparison we also show on these figures the results for a discrete homogeneous layer (solid line). The parameters for this 'equivalent homogeneous layer' were chosen by matching the area between the modulus curve and the constant substrate level and the first moment of the same area, giving

$$H_f = \frac{2\int_0^\infty (\overline{E}(x_2) - \overline{E}_s) x_2 dx_2}{\int_0^\infty (\overline{E}(x_2) - \overline{E}_s) dx_2} \tag{24}$$

and

$$\overline{E}_f = \frac{1}{H_f} \int_0^\infty (\overline{E}(x_2) - \overline{E}_s) dx_2. \tag{25}$$

The graded results show a trend similar to the homogeneous layer, but the dependence on modulus ratio is not now of power law form and both critical strain and wavenumber become less sensitive to modulus ratio at high ratios. However, the homogeneous approximation (24, 25) underestimates the critical strain by up to a factor of two and generally overestimates the corrresponding wavenumber.

Corresponding results for error-function gradation are shown in Fig. 6. The results are qualitatively similar to the exponential case, though the homogeneous approximation to the critical wavenumber is less good.

3.3 Effect of Poisson's ratio

In the preceding results, Poisson's ratio was assumed to be independent of depth. To examine the effect of grading in ν, we considered the case in which both $\bar{E}$ and ν have error function grading. In other words, $\bar{E}$ is given by (23) and

$$\nu = \nu_s + (\nu_0 - \nu_s) \operatorname{erfc}\left(\frac{x_2}{H}\right). \tag{26}$$

The critical strain and wavenumber are shown as functions of $\overline{E}_0/\overline{E}_s$ in Fig. 7 for the case where $\nu_0 = 0$ and $\nu_s = 0.49$. For comparison, we also show results for the two cases where the modulus has the same grading but Poisson's ratio is uniform and given by the extreme values $\nu_0 = 0$ and 0.49 respectively.

For a homogeneous layer on a homogeneous substrate, the critical strain and wavenumber depend only on the ratio of the plane strain moduli $\overline{E}_f/\overline{E}_s$ and are otherwise unaffected by Poisson's ratio (Huang *et al.*, 2005). By contrast, if the modulus is graded, we find a significant effect of ν even if it is assumed uniform. These effects are greatest when the modulus ratio is relatively modest. For example, for $\overline{E}_0/\overline{E}_s = 10$, the critical strain for $\nu = 0$ exceeds that for $\nu = 0.49$ by almost 90%.

The results for graded Poisson's ratio are very close to those obtained using the uniform value 0.49. In other words, a good approximation is obtained if the substrate value of ν is used throughout the body. This conclusion was verified by other numerical experiments.

3.4 Thermoelastic wrinkling

As a final example, we consider the case where the material is isotropic and homogeneous, but the fundamental stress state $\overset{0}{\sigma}$ varies with depth because of a non-uniform temperature field due to surface heating, as in Eq. (1). If the body is initially at zero temperature and the boundary $x_2 = 0$ is raised to a constant temperature T_0 for time $t > 0$, the subsequent temperature profile will be given by

$$T(x_2, t) = T_0 \operatorname{erfc}\left(\frac{x_2}{\sqrt{4\kappa t}}\right),$$

where κ is the thermal diffusivity (Carslaw and Jaeger, 1959, §2.5). The corresponding fundamental stress state is then

$$\overset{0}{\sigma}_{11} = -\frac{E\alpha T_0}{(1-\nu)}\operatorname{erfc}\left(\frac{x_2}{\sqrt{4\kappa t}}\right)$$

from (1), where α is the coefficient of thermal expansion. Both expressions have the same functional form at all times, but the characteristic length scale κt (and hence the wavelength of any wrinkles) increases with time. We can therefore determine a universal dimensionless critical thermal strain $\alpha(1+\nu)T_0^c$ and critical wavenumber $\omega^c\sqrt{\kappa t}$ from a single numerical calculation. We find

$$\alpha(1+\nu)T_0^c = 0.287; \quad \omega^c\sqrt{\kappa t} = 75.6.$$

A related problem is one in which the thermal-expansion mismatch is uniform and limited to a surface layer of thickness H_f in a homogeneous material. The critical strain for this problem is given by $\alpha(1+\nu)T_0^c = 0.267$, and the critical wavenumber is $\omega^c H_f = 12.2$. This thermoelastic problem also provides a model for other phenomena that involve compressive misfit strains within a surface layer; for example, a layer with epitaxial strains, a layer with a volume change due to a phase transition or concentration of a diffusive species (Larché and Cahn, 1982), or a piezo-electric layer. The critical strains due to pure thermoelastic effects are sufficiently large that the surface instabilities may not be of practical significance when there is no modulus mismatch, but in conjunction with a stiff surface layer, phenomena such as thermoelastic wrinking are likely to occur at practical levels of strain.

4 Conclusions

We have presented a general strategy for determining the critical strain and the corresponding wavenumber for the wrinkling instability of a half space or thick layer loaded in compression, when the elastic properties vary with depth. Results exhibit dependence on modulus ratios similar to those observed when a homogeneous stiff surface layer is bonded to a more flexible substrate (i.e. where the elastic properties are piecewise constant). We present expressions permitting analytical results for the latter case to be used in an approximate sense. The method can also be applied to thermoelastic loading associated with transient surface heating and we give results for the critical surface temperature at which a homogeneous half space will develop wrinkling.

Acknowledgements

This work was supported in part by NIH (EB003793-01).

References

Bowden N, Huck WTS, Paul KE, Whitesides GM. The controlled formation of ordered, sinusoidal structures by plasma oxidation of an elastomeric polymer. Applied Physics Letters 1999;75:2557–2559.

Budiansky B. Theory of buckling and postbuckling behavior of elastic structures. Advances in Applied Mechanics 1974;14:1–65.

Carslaw, H.; Jaeger, JC. The Conduction of Heat in Solids. 2nd. Clarendon Press; Oxford: 1959.

Chen X, Hutchinson JW. Herringbone buckling patterns of compressed thin films on compliant substrate. ASME J Appl Mech 2004;71:597–603.

Efimenko K, Rackaitis M, Manias E, Vaziri A, Mahadevan L, Genzer J. Nested self-similar wrinkling patterns in skins. Nature Materials 2005;4:293–297.

Huang ZY, Hong Z, Suo Z. Nonlinear analyses of wrinkles in a film bonded to a compliant substrate. J Mech Phy Sol 2005;53:2101–2118.

Koiter, WT. Delft Univ Thesis in Dutch [NASA Tech Transl in 1967, TT F–10]. 1945. On the stability of elastic equilibrium; p. 833

Larché FC, Cahn JW. The effect of self-stress on diffusion in solids. Acta Metall 1982;30:1835–1845.

Moon MW, Lee SH, Sun JY, Oh KH, Vaziri A, Hutchinson JW. Wrinkled hard skins on polymers created by focused ion beam. PNAS 2007;104:1130–1133. [PubMed: 17227839]

Stafford CM, Harrison C, Beers KL, Karim A, Amis EJ, Vanlandingham MR, Kim KC, Volksen W, Miller RD, Simonyi EE. A buckling-based metrology for measuring the elastic moduli of polymeric thin films. Nature Mater 2004;3:545–550. [PubMed: 15247909]

Triantafyllidis N, Peek R. On the stability and the worst imperfection shape in solids with nearly simultaneous eigenmodes. Int J Solids Struct 1992;29:2281–2299.

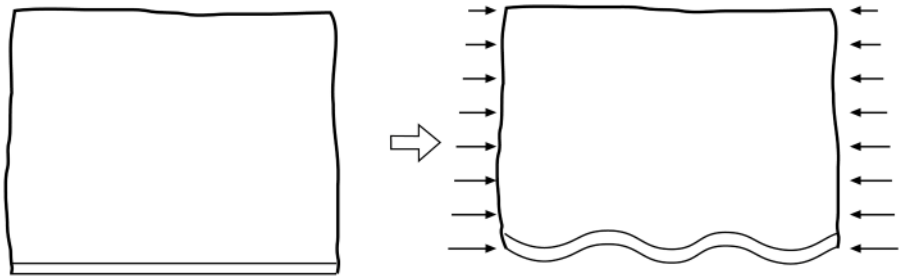

Fig. 1.
Schematic of a half space subjected to a compressive load

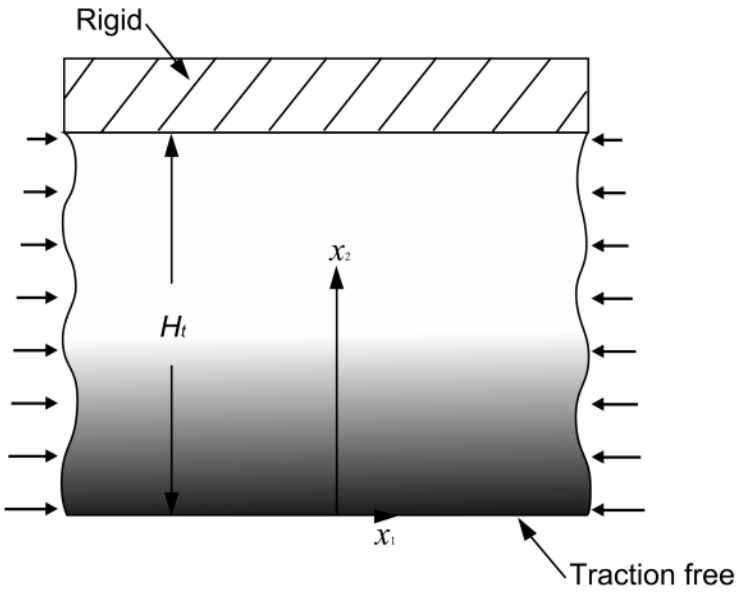

Fig. 2.
The graded layer subjected to a compressive load

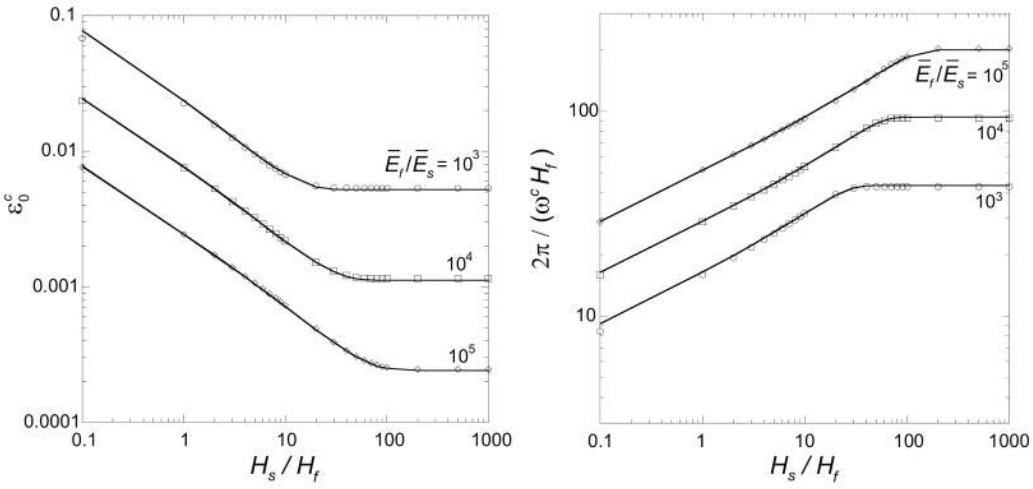

Fig. 3.
Critical strain and wavelength for a homogeneous layer on a dissimilar substrate. The solid lines are taken from Huang *et al.* (2005).

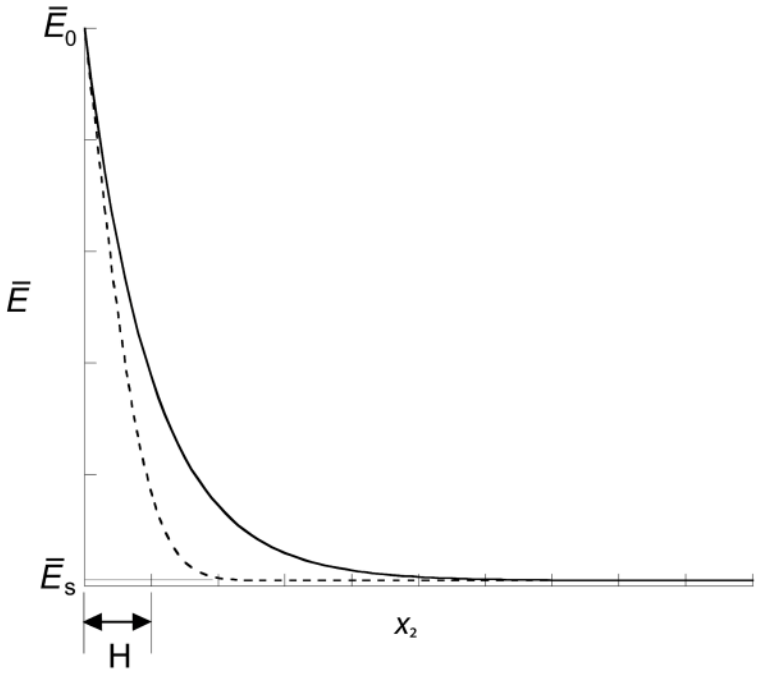

Fig. 4.
Examples of variable modulus: — exponential grading, - - - error function grading

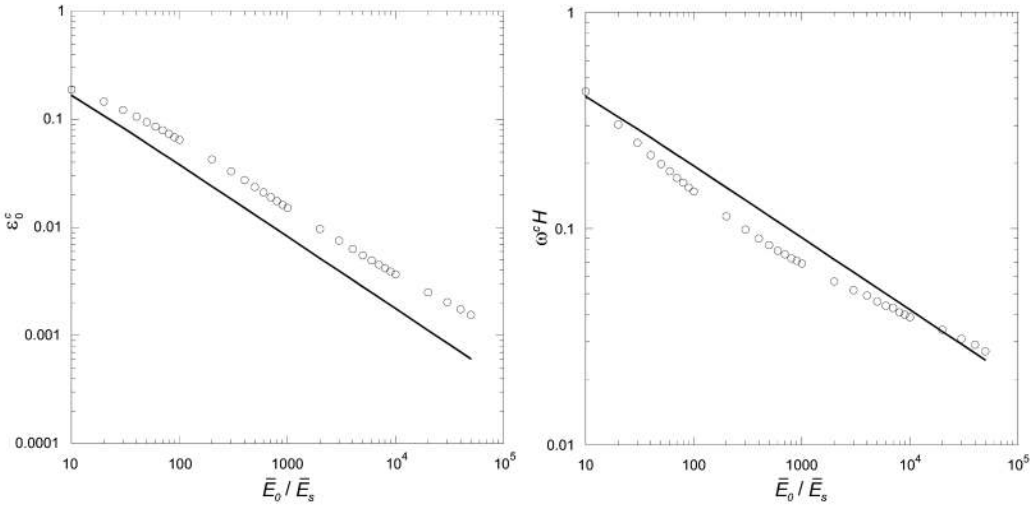

Fig. 5.
Critical strain and dimensionless wavenumber for exponential grading. The solid line represents a homogeneous layer approximation using equations (24, 25).

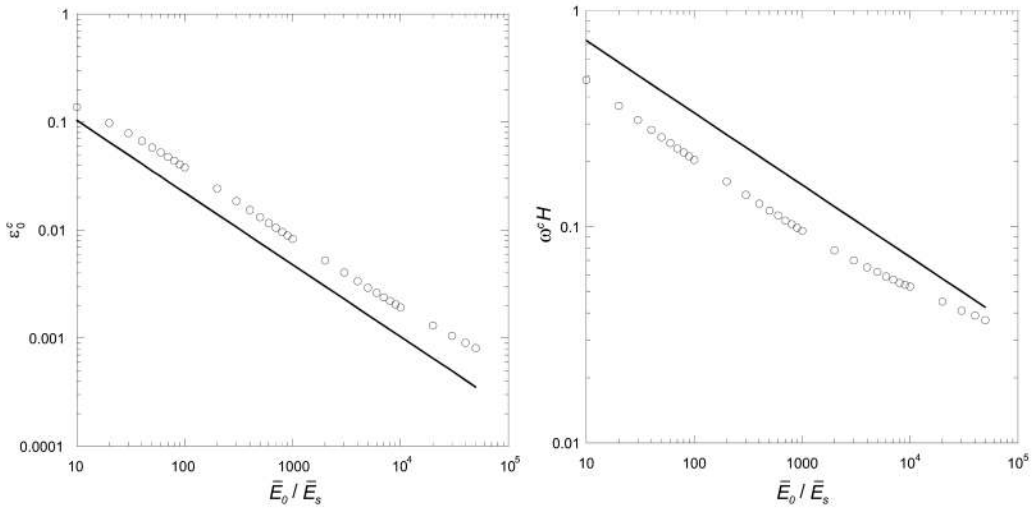

Fig. 6.
Critical strain and dimensionless wavenumber for error function grading. The solid line represents a homogeneous layer approximation using equations (24, 25).

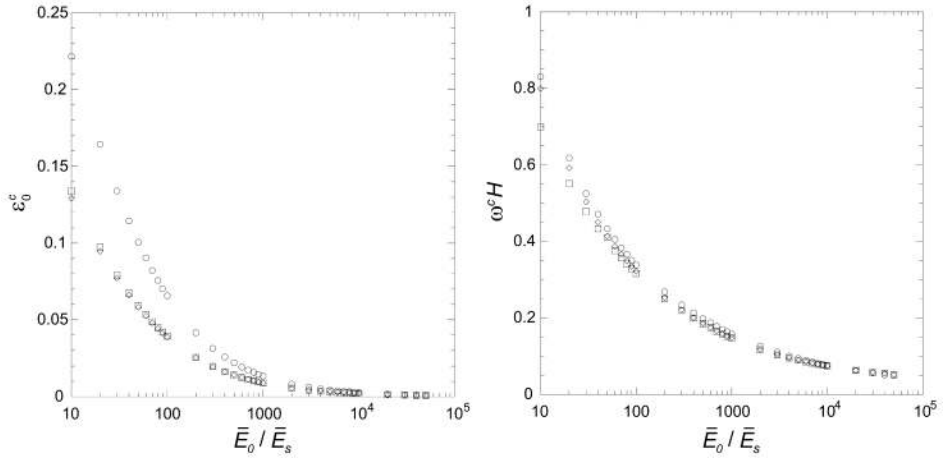

Fig. 7.
Effect of Poisson's ratio: (○) $\nu = 0$ and uniform, (□) $\nu = 0.49$ and uniform, (◊) Eq. (26) with $\nu_0 = 0$, $\nu_s = 0.49$.